INDIVIDUAL PROGRESS REPORT

ALEX SUCHKO – OCTOBER 26TH 2011

GROUP #1

TABLE OF CONTENTS

1. Introduction

1.1. Overview

Our overall project is to develop a mobile robot capable of producing vector graphics using common, off the shelf chalk. This semester our focus is to develop electronic control hardware for the robot. Production services and materials for the manufacture of the mechanical platform, including drive motor sets, were donated use in our project by *ECU, inc*. Software demonstrating basic robot operation will be demonstrated at the close of this semester.

FIGURE 1 – OWN WORK

Please note that the ISO 690 Numerical style of citation is used in this document. Sources have been enumerated at the end of this document, and are referenced throughout by their index, i.e. "(n)", where n is the index number of the source.

1.2. Personal Individual Parts

In section two, I have summarized parts of the project for which I have been responsible as of the writing of this document. For efficient use of space, I have not re-listed them here. Please refer back to the table of contents on the previous page for a listing of topics and their associated starting page numbers. In particular, I worked on the robot mechanical platform, a study of PWM frequency selection for drive motor control, component value design for a switching buck mode power supply (PSU), testing for our H-Bridge module, specification of ultrasonic distance sensors for peripheral object sensing, specification of a processor to use for motion control, and design of the robot control sections of the carrier board.

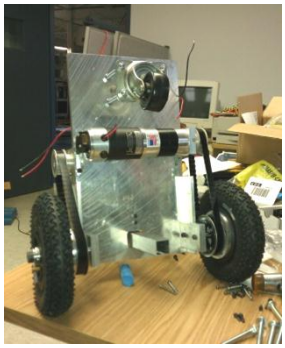

FIGURE 2 – OWN WORK

2. Individual Parts

2.1. Robot Mechanical Platform (GoBot)

2.1.1. Brief Overview

After several design iterations, including something akin to a drive-around Cartesian robot, we arrived at the platform we now see today. The platform consists of two driven rear tires with a forward mounted un-driven caster wheel. A chalk feed mechanism is mounted with the chalk center on the axis of the rear drive tires, midpoint between the drive tires. This geometry ensures that the chalk naturally travels tangent to the robot's direction of travel, mimicking the action used by a human artist.

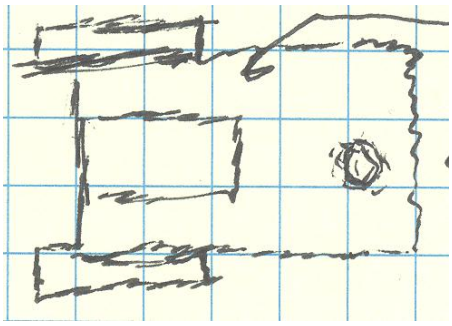

2.1.2. Motor Selection

After massing the robot, I did some calculations to arrive at the needed mechanical output specifications for the drive motors (one is seen in Figure 2).

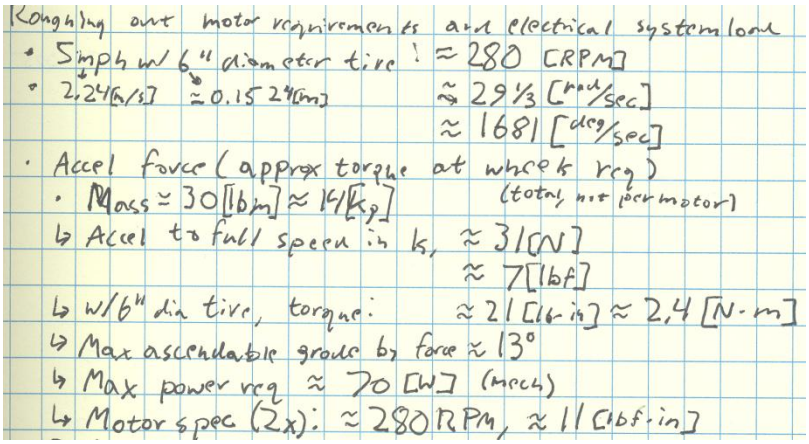

The final results of interest as seen above resulted in requirement of a 280[RPM], 11[lbf-in] continuous duty motor. George (1) and I had previously discussed brushless motors (electronic commutation), but due to the level of complication of our project as a whole, we decided to use brushed motors (mechanical commutation) to ease the design load. A brushless motor would require a triple-half-bridge type inverter to drive what is essentially the three-phase permanent magnet AC motor. A brushed motor on the other hand requires only a DC input, with the AC inversion handled by internal mechanical contacts ('brushes').

Ultimately, a Midwest Motion Products D22-376D-24V GP52-016 EU-100 (2) brush type motor was selected, (shown in Figure 2). This 24v gear-motor set includes a brushed 24v motor, planetary gear drive, and optical quadrature encoder already assembled together. The purchase of these motors was made possible by *ECU, inc*. Note, though designed to operate up to 24v, our system voltage is 12v (discovered full torque was not necessary during remotely operated robot test drive).

The encoder resolution of 100[PPR] was selected for three reasons. First, any higher resolution made no sense as this was beyond the mechanical accuracy of the gear drive at it's output. Second, a high resolution (after gear drive, resolution at output shaft is 1588[PPR]) was desired to attain reasonable 1st and 2nd time derivative resolution from encoder data so that position, velocity, and acceleration of the motors can be sensed. Finally, the output frequency of this encoder at the maximum design motor RPM was within the acceptable range for a hardware quadrature encoder interface (at it's heart, an up/down counter with a d-latch to make the up/down signal persist).

2.1.3. Battery Selection

Due to the high percentage of total system electrical load represented by the motors, this estimation had to be completed prior to the selection of a battery for our mobile robot.

FIGURE 3 - POWER SONIC

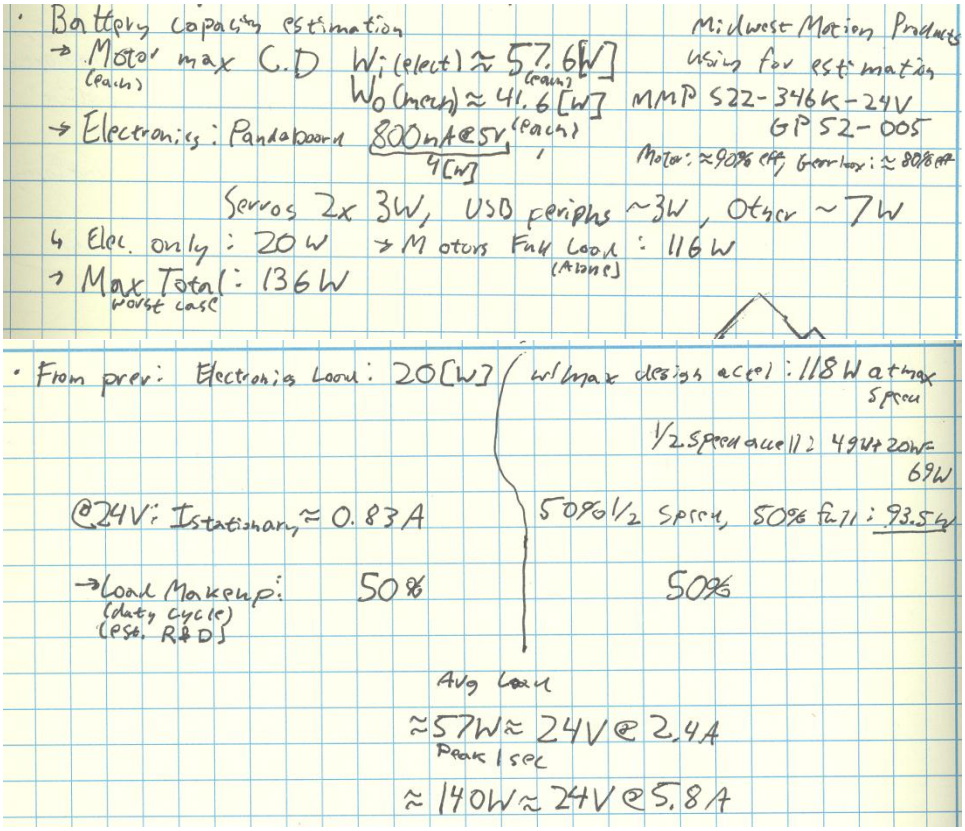

We initially considered using an exotic battery type, perhaps Li+ or $LiFePO_4$ (A123 systems) cells. Once we decided to change the system voltage from 24v to 12v, *ECU, inc.* was able to provide us with a sealed $Pb\text{-}H_2SO_4$ (3) (Lead-Acid) type battery free of charge for the duration of this project. The battery provided was a Power Sonic PS-1270, a 12v nominal, 54W-h battery (4), pictured in Figure 3.

2.1.4. Final Design

The chalk mechanism was designed and manufactured by the *ECU, inc.* shop. It utilizes a pair of hobby servos for actuation, one is used to change the height of the chalk tube, the other is used to lock and unlock the chalk to the tube (not pictured in Figure 4). The clever belt drive adapter for the drive tires was designed jointly between *ECU, inc.* and I.

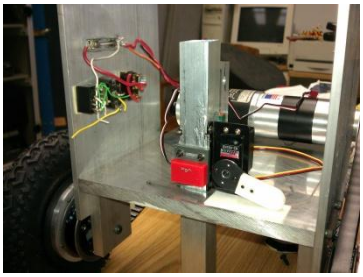

FIGURE 4 - OWN WORK

Other factors were designed and/or considered in the development of the mechanical platform, which have been omitted for brevity, as this document has a length restriction.

2.2. Study of PWM Frequency Selection for Drive Motor Control

2.2.1. Minimum Frequency

What led to the discovery of a criteria for the minimum reasonable PWM switching frequency for H-bridge type control of a brushed DC motor started as a study of what was the optimal frequency for PWM control.

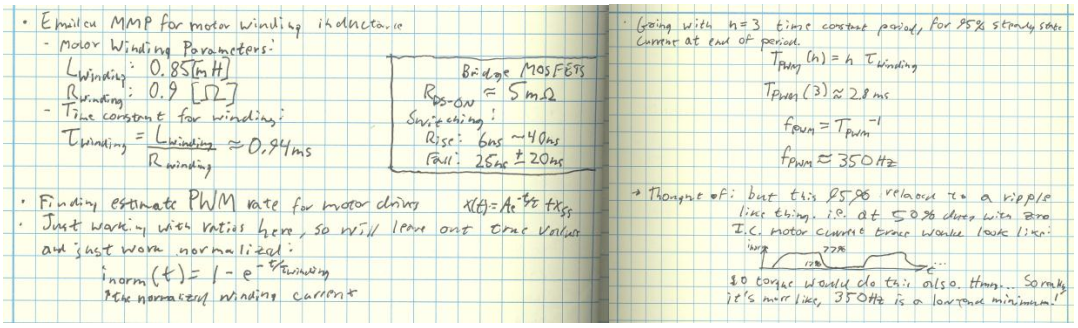

As is shown in my calculations and notes above, it is important to note that this current rise and fall on the PWM edges translates to a torque ripple. Meaning, it is important that the PWM period not be longer than a few time constants of the motor winding (and drive) circuit to avoid saturation, but it is also important to consider smoothness of torque output (this also involves an evaluation of the mechanical dynamics intrinsic to the motor and those of the attached system to thoroughly evaluate).

2.2.2. Maximum Frequency

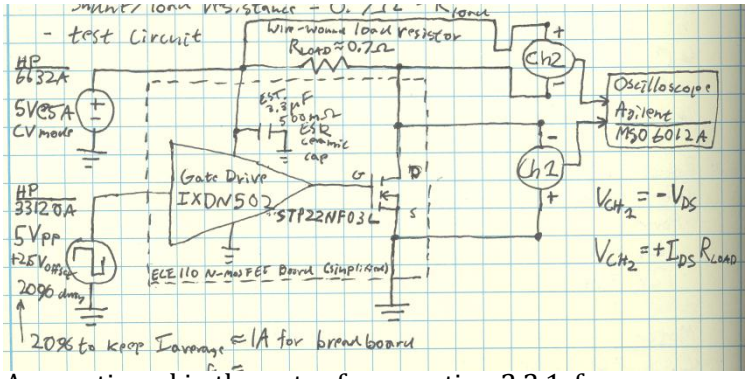

FIGURE 7 - OWN WORK

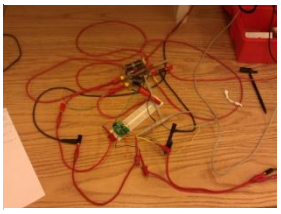

FIGURE 6 - OWN WORK

As mentioned in the notes from section 2.2.1, for our purposes heating was the only upper bound considered. To estimate heating, we set up an experiment using a low-side drive board used in the ECE 110 lab, pictured in Figure 7 which uses a low side drive strategy similar to the one used in our H-Bridge module. Our test setup is shown schematically below from my notes, and physically in Figure 6 (instrumentation not shown).

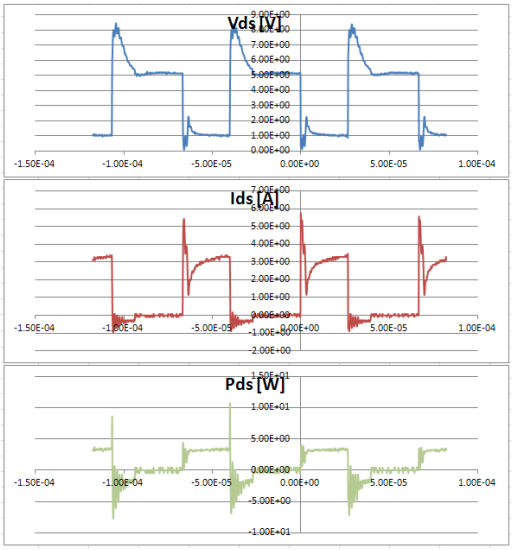

FIGURE 5

Our test results ultimately proved 'inconclusive' due to a larger than expected inductance present in the wire-wound resistor we used as a current shunt (sample 150kHz data shown left in

Figure 5, note nonsensical negative values on I_{ds}, P_{ds}). Nonetheless, our results found that at 3kHz, all components produced significantly less heating than at 20kHz, and operated with an acceptable temperature rise. Prior to George carrying out thermal performance calculation on the H-Bridge module, we used 3kHz as our accepted switching frequency when needed for calculations.

See George's work on the H-Bridge module for further information regarding thermal performance calculation for our final design.

2.2.3. Optimal Frequency

Many quanta can be considered when choosing the 'optimal' switching frequency. In our case, we originally wished to switch at an ultrasonic frequency (i.e. above 20kHz), but at present we have decided to use a switching frequency in the neighborhood of 3kHz, yielding mitigated torque ripple with acceptable heating loss due to switching, and an acceptable audio emission.

2.3. Switching Buck Mode Power Supply (PSU)

2.3.1. Component Selection

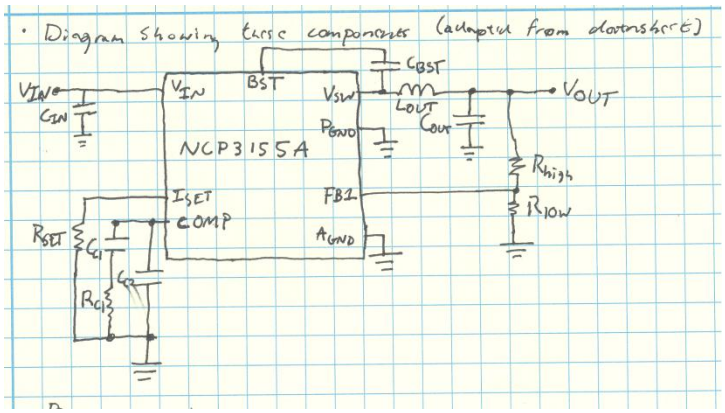

I performed the component design for our NCP3155A based buck mode switching power supply, designed to take 12v nominal as input and provide a stable 5v output at about 1.5A max. George developed the schematic and PCB design. The NCP3155A datasheet was used for design equations and reference throughout the component design process (5). This power supply design will be used to provide regulated electrical power for the the Panda board, carrier board, and chalk actuation servos. Not mentioned here, the INA226 mounted onboard enables the supervisor/reset sequencer processor board to monitor performance of the supply design at it's output (voltage, current, power) via I^2C bus.

Design Parameters		Values to design		
V_{IN}	9v-16v, nom. 12v	General	C_{OUT}	Output capacitance
V_{OUT}	5v		C_{IN}	Input capacitance
V_{IN_RIPPLE}	300mV		L_{OUT}	Output inductance
V_{OUT_RIPPLE}	50mV		R_{SET}	Current limit set R
I_{OUT}	1.5A		C_{BST}	Bootstrap capacitor
F_{SW}	500kHz	Compensation	C_{C1}	Compensation cap 1
			R_{C1}	Series R for C_{C1}
			C_{C2}	Compensation cap 2
		Feedback Sense	R_{HIGH}	High sense divider R
			R_{LOW}	Low sense divider R

Highlights from component design

Much of the component design has been left out of this document due to space constraints. Please see my design notebook for full details on the calculation of values for all support components.

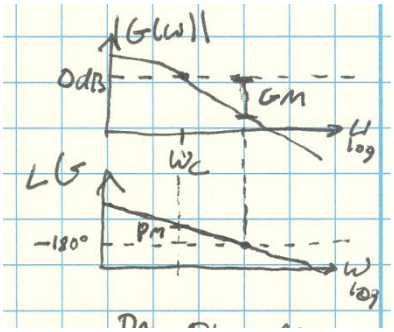

I have chosen to include information regarding calculations for the compensation network, since it's one of the most nebulous components in the design. The compensation network is in place to improve the phase margin (6) of the error amplifier in the NCP3155A. Without the compensation network, when observing the performance of the feedback control in the frequency domain the phase of the system drops below -180° at frequency lower than that at which the gain drops to 0dB (the crossover frequency), meaning the system is unstable.

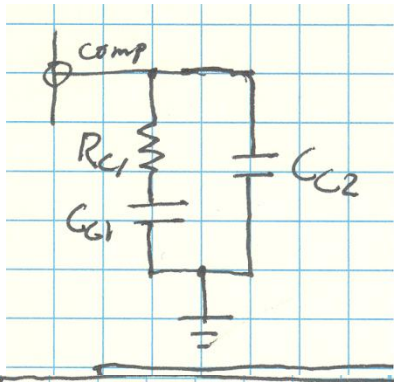

The RC compensation network is used to boost the phase of the controller, allowing stable operation.

Running these calculations, we arrive at the values for the three compensation components listed in the table below. As the capacitance values are tiny, I chose to run calculations to find what approximate capacitance contributions I could expect from the PCB traces, using a parallel plate capacitor approximation. These values ended up being 1 to 2 orders of magnitude below the compensation network values. However, you touch your finger to the compensation network, you do vary the values enough by adding your own capacitance to cause instability. For this project this semester this was deemed not enough of a problem to force revision.

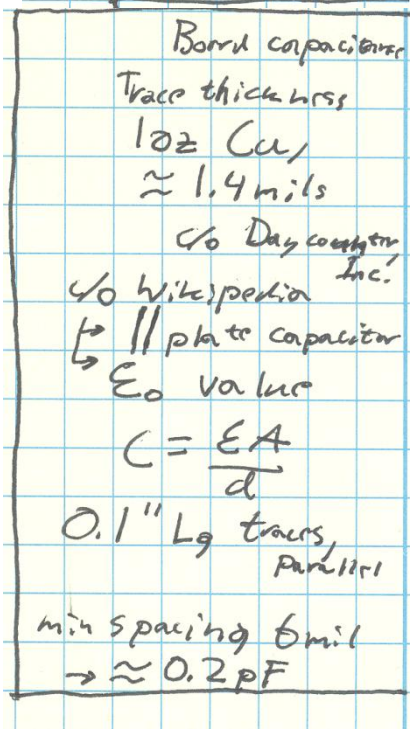

It is important to note that R_{SET} was originally calculated to be about 10kΩ, resulting in a current limit of about 2.6A. However, during testing it was found that the current limiting was unstable, so the current limit was defeated by removing R_{SET} (approximately infinite resistance).

Values as built		
General	C_{OUT}	22µF
	C_{IN}	22µF
	L_{OUT}	22µH
	R_{SET}	∞Ω
	C_{BST}	0.1µF
Compensation	C_{C1}	165pF
	R_{C1}	178kΩ
	C_{C2}	3.6pF
Feedback Sense	R_{HIGH}	19.6kΩ
	R_{LOW}	3.74kΩ

2.3.2. Debug and Testing

Initially found that a IRF9317 P-FET, used as a high side enable switch for our NCP3155A implementation, had been placed backwards in the schematic. We devised a hack and fixed it on the fly involving snipping pins, electrical tape, and jewelry wire Figure 8.

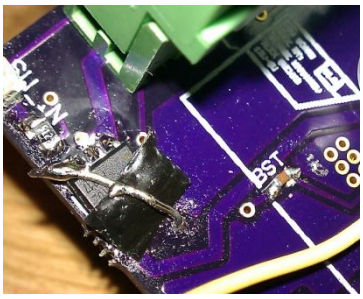

FIGURE 8 - OWN WORK

Test setup shown at right.

Note: HP E3631A was later changed out for HP 6632A when it was discovered E3631A was not regulating transient current draws from switching supply well (transient load near current limit).

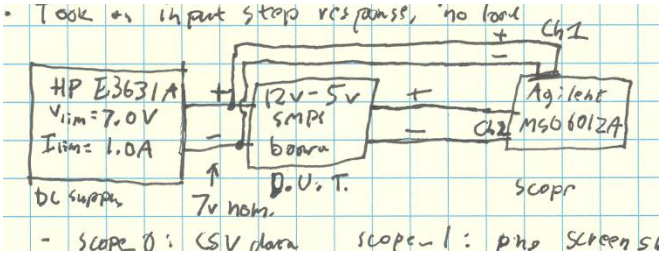

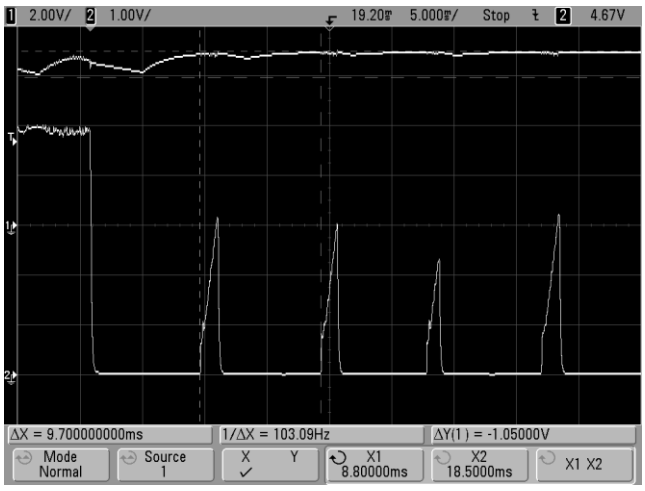

FIGURE 9

Later found power supply shutting down randomly, shutting down when step load applied of about 1.8A. Tried a number of permutations, eventually discovered that current limit was tripping prematurely. Current limit uses DS junction in high side n-fet within the NCP3155A (internal switch) as a current shunt. Something is spooking overcurrent detect. Feature not necessary for us, disabled by

removing R_{SET}. Problem was recognized when scope the strange periodicity in trace Figure 9, channel 2 (lower trace) was observed during supply malfunction (matched a scope trace found in datasheet of current limit functioning). Removing R_{SET} corrected issue, enabling stable operation. Also fixed issue with failure to start on fast V_{IN} rise rate. Performed a load test on supply, results listed below. Note that supply shorted shortly after test ended, likely due to stress during removal of R_{SET}.

Input	V_{IN}	15V
	I_{IN_AVG}	0.438A
	P_{IN_AVG}	6.57W
Output	V_{OUT_APPROX}	5V
	I_{OUT_APPROX}	1.25A
	P_{OUT_APPROX}	6.25W
Efficiency	$P_{DISSIPATION\_APPROX}$	0.32W
	$\%_{EFFICIENCY}$	95%

In a later test with a similar output load, this time about 6.9W, the $V_{PP\_OUT\_RIPPLE}$ was measured to be about 265mV, at a fundamental frequency of about 510.20kHz (≈F_{SW}, ideally 500kHz), these quanta are highlighted in Figure 10, note that channel 2 (green) is the output voltage.

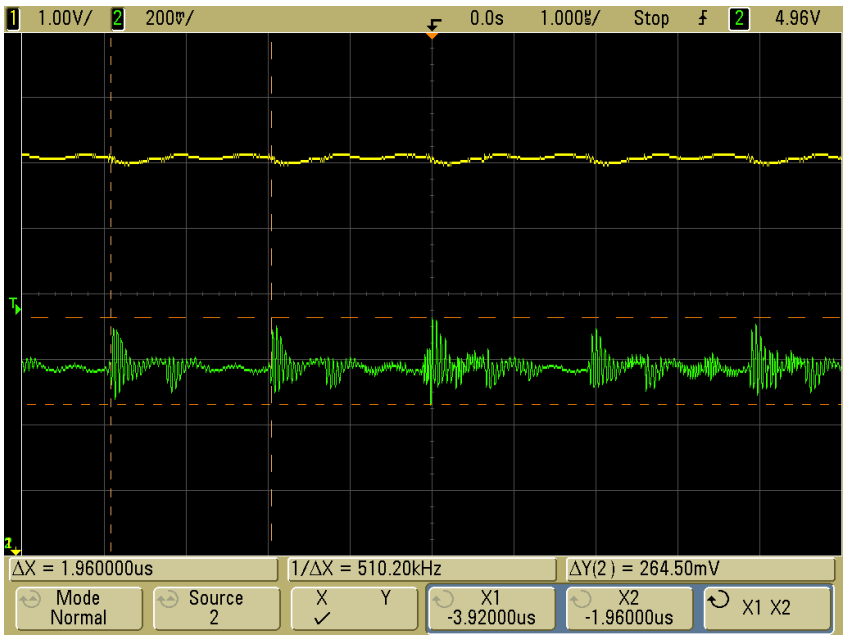

FIGURE 10

2.4. H-Bridge Testing

2.4.1. Test Setup

Testing of our H-Bridge design was performed using an ECE 110 car. This was selected as the ECE 110 car has a battery which is often around 10v and has quite a bit of internal resistance, giving a good 'worst case' old battery situation, large input voltage dips PWM duty cycle start (rising edge). Also, the drive motors on the ECE 110 cars are known to be electrically noisy, and can easily be loaded by applying friction to the ECE

110 car's drive tires. Both motors run in parallel give a load that is analogous in current to one of our drive motors on the actual robot.

A picture of the physical setup is given in Figure 11. The schematic follows below. Note that the Teensy, something like an Arduino, has been programmed to output a 3kHz, 20% duty PWM signal to the PWMH line on the H-Bridge. It is also monitoring the FF1 and FF2 lines for faults, and will light an LED if one is detected.

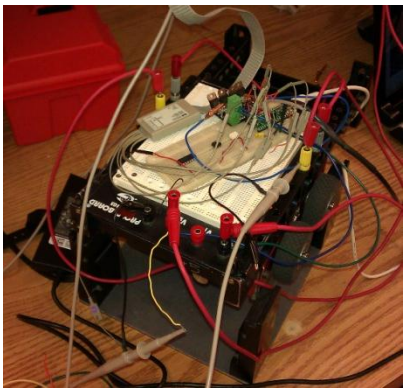

FIGURE 11 - OWN WORK

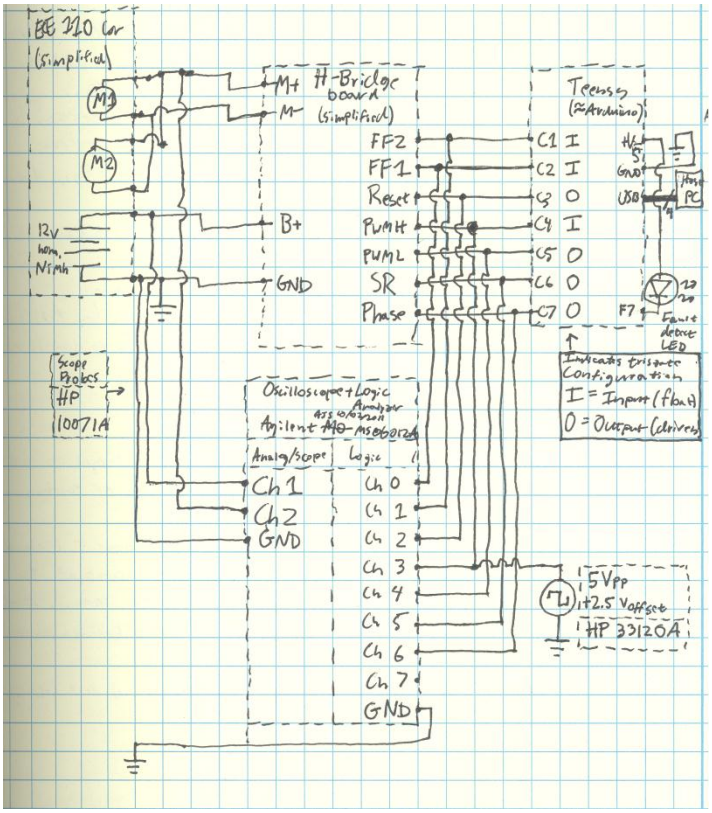

2.4.2. Results

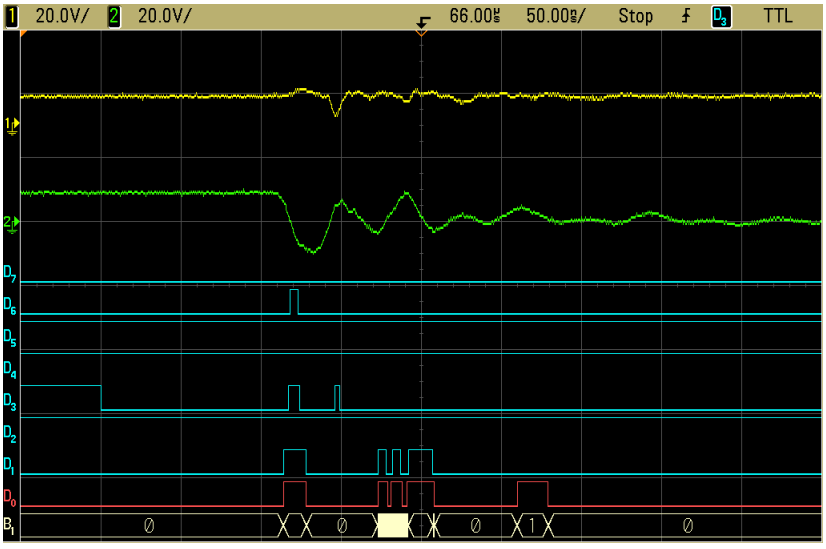

FIGURE 12

H-Bridge operates, but occasional erroneous fault detections by Teensy programmed to detect fault codes on FF1, FF2 lines from H-Bridge. After taking scope traces and looking closely at what occurs around edges on the PWM input, it can be seen that noise from the power bridge is intruding at significant levels into logic signals, causing false 1s and 0s on logic lines. Figure 12 shows the undesired transients on logic lines following a falling edge on the PWMH input (as shown in setup schematic in 2.4.1, D_3 is the PWMH line, and can be seen going low about 50ns from the left side of the trace).

Note there should be no digital line state changes visible other than D_3 going low here, all other pulses are undesired. Also, note the extreme voltage swing on the motor terminal (channel 2, green), which dips as low as about -10V at one point, going past 0V and continuing to -10V in approximately 25ns, clearly synchronous rectification (SR) is not catching this in this short time scale, and the body diode is being overwhelmed.

Found that design of H-Bridge did not separate power bridge and logic signal grounds, encouraging noise intrusion into logic level signals from power bridge. Decided to make some changes and design a new revision of H-Bridge design to abate some noise. New revision added 0.1µF capacitors across each DS junction on power bridge MOSFETs, reduces high frequency transients. Provisioned for adding series resistance into gate drives to control slew rate on MOSFETs. Added external supplementary flyback diodes across DS junctions to improve very high frequency (fast) transients that occur before body diode or synchronous rectification respond during gate-off (ns time scale after falling edge on PWM input signal).

Though no quantitative temperature rise testing was done, qualitatively the power bridge MOSFETs remained cool to the touch throughout testing, less dissipation than had been estimated by George's calculations.

2.5. Ultrasonic Safety Sensors

2.5.1. Principle of Operation

Time-of-flight distance measurement is used in our project to detect approaching objects for safety functions on the robot. One sensor each is mounted on the front, back, left, right sides of the robot. For example, if an asteroid has landed in the region where a drawing is to be produced, the ultrasonic sensor array can detect the extraterrestrial visitor and stop before crashing.

FIGURE 14 - PARALLAX, INC.

Or, perhaps a curious person walks up to look at the robot and we want to avoid hitting them by stopping, improving the safety of the public in keeping with the first point of the IEEE Code of Ethics (7). It is important to note that though additional safety features have been specified for the robot, such as ultrasonic peripheral object detection, robot mass and speed do not constitute a significant risk of serious injury.

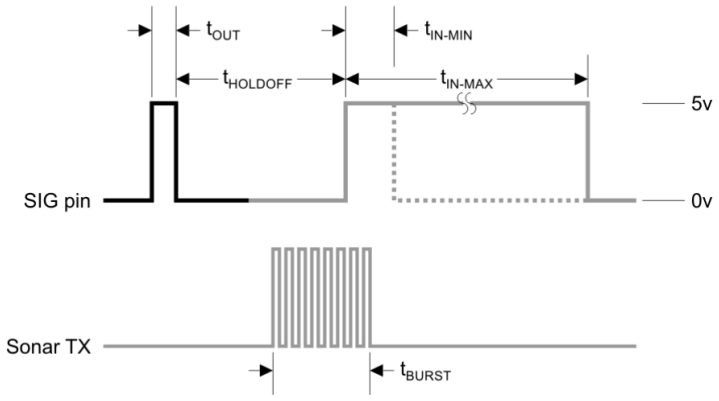

FIGURE 13 – PARALLAX, INC.

Ultrasonic time-of-flight distance measurement is accomplished by sending a chirp, in the case of the Parallax PING))) sensor (Figure 14) 40kHz, of sound waves into a medium, and timing how long it takes for them to reflect back. Since the speed of wave propagation in a medium such as air is know fairly well, the distance to an object can be calculated from the chirp's time of flight.

2.5.2. Signaling

Most signal generation and processing is performed on-board the PING))) sensor board. A simple digital interface is provided to the user, which takes advantage of tri-state buffers. The user starts by driving a keying pulse to the PING))). The user then turns the line around, and the PING))) drives a pulse high about 75% through the transmission of the chirp, which remains high until the first (important, makes life easier) echo is received, or until 18.5ms elapse, whichever comes first. This last feature keeps you from getting stuck in receive. A diagram of this signaling process is provided in Figure 13 (8).

2.6. Motion Control Processor

2.6.1. Reasoning for Selection

Motion control processor handles interfaces with many sensors giving information about the current state of the robot, including ultrasonic sensors, quadrature encoders, and inertial measurement unit. Outputs are issued to the H-Bridge modules for the left and right motors, and to the two chalk actuation servos and any accessory loads via the two accessory low side drives. The motion control processor is located on the carrier board.

Originally, planned on using ST Microelectronics STM32F105 processor for motion control processor. However, parts shop here is not able to mill traces fine enough to support reliable fan-out from STM32F105, whose friendliest package is an LQFP-64. We considered making a board to be sent out, but time constraints proved an issue for turnaround time. Ultimately, we chose to use part of our coupon from Texas Instruments from the Engibous design contest to purchase an EKK-LM4F232, internally named Armadillo. This is a development board for the fastest ARM Cortex-M4 based processor in the Stellaris line that Texas Instruments has available. However, most importantly in our case, it has nicely laid out (pins in a logical order) 0.1" spaced through holes in which we can solder header pins.
The LM4F232 in an LQFP-144 package mounted on the Armadillo board exceeds all I/O and peripheral requirements for the motion controller. Note that this table has been updated to match the hardware as it was laid out on the carrier board.

Peripheral Type	Channels Required
GPIO	17
ADC	2
PWM	4
Quadrature Encoder Interface (QEI)	2
Input Capture	4
I^2C	2
USB	1

2.6.2. Pin Mapping

Pin mapping is necessary to route connections from appropriate peripherals through pins and ultimately to control or sense the appropriate circuit nets/nodes. Below is the mapping table listing routing that achieves these goals, and provides an optimized PCB layout (minimizes crossing traces, vias).

Feature Set	Signal	LM4F232 Pin	Direction
Ultrasonic Sensor	US_BUFFER_DIR	PL4	O
	US1_SIG	PL0	I/O
	US2_SIG	PL1	I/O
	US3_SIG	PL2	I/O
	US4_SIG	PL3	I/O
Chalk Switch	CHALK_SW	PJ0	I
I^2C	HBR_SCL	PB2	I/O
	HBR_SDA	PB3	I/O
	IMU_SCL	PA6	I/O
	IMU_SDA	PA7	I/O
QEI	QEI_1_B	PC6	I
	QEI_1_A	PC5	I
	QEI_1_INDEX	PC4	I
	QEI_2_B	PF1	I
	QEI_2_A	PF0	I
	QEI_2_INDEX	PF4	I
H-Bridge	HBR_LEFT_FF2	PN4	I
	HBR_LEFT_FF1	PN3	I
	HBR_LEFT_RESET	PD4	O
	HBR_LEFT_PWMH	PD1	O
	HBR_LEFT_PWML	PD3	O
	HBR_LEFT_PHASE	PD2	O
	HBR_LEFT_ALERT	PN2	I
	HBR_RIGHT_FF2	PN7	I
	HBR_RIGHT_FF1	PN6	I
	HBR_RIGHT_RESET	PD7	O
	HBR_RIGHT_PWMH	PD0	O
	HBR_RIGHT_PWML	PD6	O
	HBR_RIGHT_PHASE	PD5	O
	HBR_RIGHT_ALERT	PN5	I
Servo (SVM)	SVM_1_SIG	PH2	O
	SVM_2_SIG	PH3	O
Accessory	ACCY_1	PH1	O
	ACCY_2	PH0	O

2.7. Carrier Board (Motion Control, Feedback, Sensing)

2.7.1. Circuit Design

2.7.1.1. 5v and 3.3v Power

Sourcing 5v and 3.3v power for the carrier board proved to be an interesting venture. As it is now, there are three 5v domains and two 3.3v domains on the carrier board.

Domain Voltage	Source	Supplied Loads
5v	PSU1	Pandaboard, Armadillo (aka Motion Controller) (via Pandaboard), Carrier board interfaces, Quadrature encoder power
	PSU2	Servos
	Linear	Supervisor
3.3v	Armadillo	Carrier board logic, IMU
	Supervisor	Internal functions only

An additional regulator was considered on the carrier board for 3.3v logic regulating from 5v, but after calculations related to the Armadillo's (9) (motion controller, EKK-LM4F232) 3.3v regulator (10) it was found that sufficient 3.3v power could be sourced from the onboard regulator to support both the Armadillo and external carrier board circuitry.

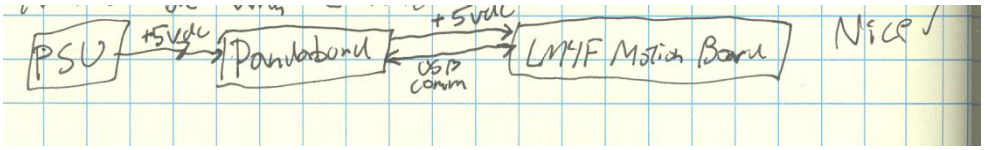

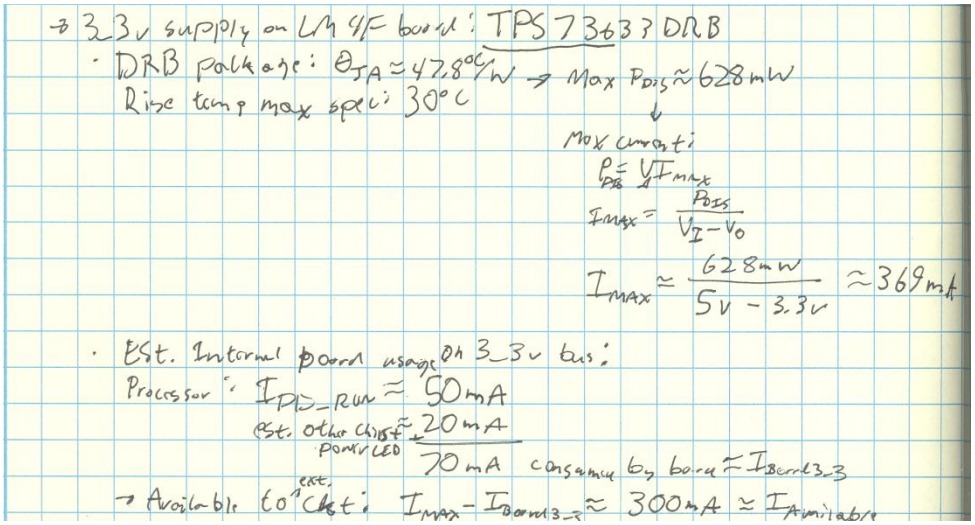

2.7.1.2. Ultrasonic Sensor Interface

Before reading this section, it may be helpful to first review section 2.5 for a high-level view of how the ultrasonic sensor works. The major interfacing issue between the Armadillo and the ultrasonic sensor is the logic level: the Armadillo is a 3.3v device, while the ultrasonic sensors have 5v logic.

A bi-directional logic level translator (11) capable of translating between 5v and

3.3v logic was selected to interface between the two. Before running out to the header pins which will be used to connect to the individual ultrasonic sensors, I decided to put a resistor in series with each, R_{SAFE}. This resistor's value was calculated such that if a signal line were to accidentally be exposed to a battery cable, the resistor would limit the current. The limited current was calculated such that the intrinsic diode in the logic level translator would be able to withstand this condition long enough to guard against an errant brush with a battery positive cable. R_{SAFE} as shown below was calculated to be about 140Ω, but was ultimately specified as anywhere between 140Ω and 150Ω to use standard/available values as this specification is not exacting.

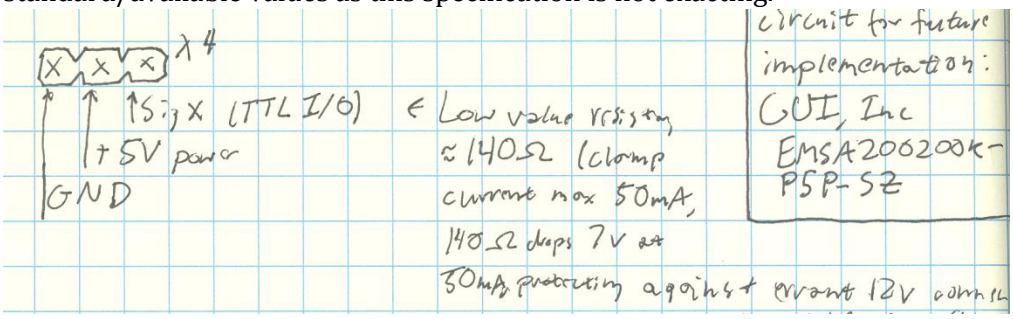

2.7.1.3. I²C

Two I²C channels are used out of the Armadillo. One is simple, running to the IMU board which houses the I²C pull-ups for the line as well as a level translator on-board, so traces only needed be run from the appropriate pins to the IMU.

The other is a bit more complicated. The I²C channel used to communicate with the power monitors (12) on the H-Bridge board must level translate to a 5v bus voltage from the 3.3v bus voltage used by the Armadillo. This was accomplished via use of a level translator (13). With appropriately selected support components, this device bi-directionally translates the open-drain I²C bus level between the Armadillo and H-Bridge power monitors.

2.7.1.4. PWM Outputs

Please see section 2.6.2 for a mapping of PWM signal outputs. Two of these outputs run at about 3kHz, and are routed to the two H-Bridge PWMH lines, the other two are run at about 50Hz with a pulse width of about 800µs to about 2200µs to issue control signals to the chalk actuation signals.

All PWM outputs needed 5v logic levels, and were run through the same logic level translators as mentioned in section 2.7.1.2 (11), except that the direction lines never need to be changed from output to input, so they have their direction lines pulled with a resistor to remain in output mode. R_{SAFE} has been left off these lines as future work may require these lines to drive optically isolated inputs.

2.7.1.5. Limit Switch (Chalk Switch)

A limit switch is installed on the chalk mechanism to signal when the chalk is low. Interface with this sensor is accomplished by pulling one side of the switch high with a resistor R_{PU} = 10kΩ. The other side of the switch attached to ground, so that when the switch closes, the signal transitions from near V_{DD} to near GND.

R_{SAFE} was also included to protect the LM4F232 (Armadillo). Note that when the switch is closed a resistor divider is formed by R_{PU} and R_{SAFE}, though R_{SAFE} is orders of magnitude more conductive so the logic level is still sufficiently low when the switch is closed.

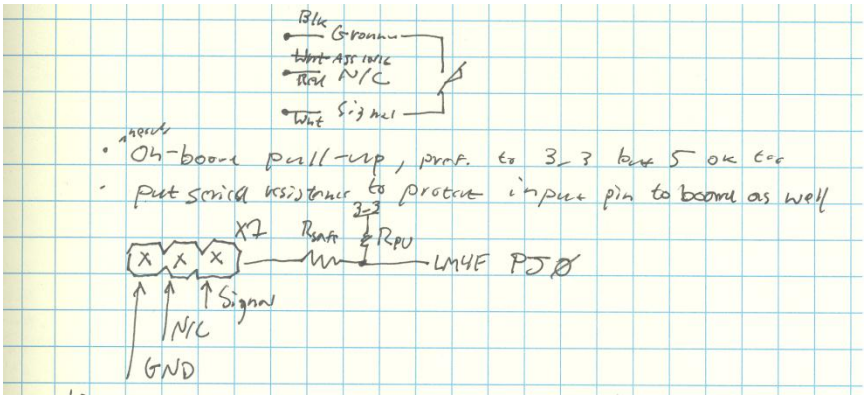

2.7.1.6. Quadrature Encoder Interface (QEI)

For information on pin-out to the Armadillo from both QEI channels, please see section 2.6.2. Both channels provide 5v power to the QEI, and read back three 5v logic pins: Phase A, Phase B, and the Index signal. A principle of operation for quadrature encoders is not included here due to length constraints on this document, but is available upon request.

The logic level on these lines is 5v, but a logic level translator is not necessary as all pins on the LM4F232 (Armadillo) when in input mode are 5v logic tolerant (can accept up to 5v without problem).

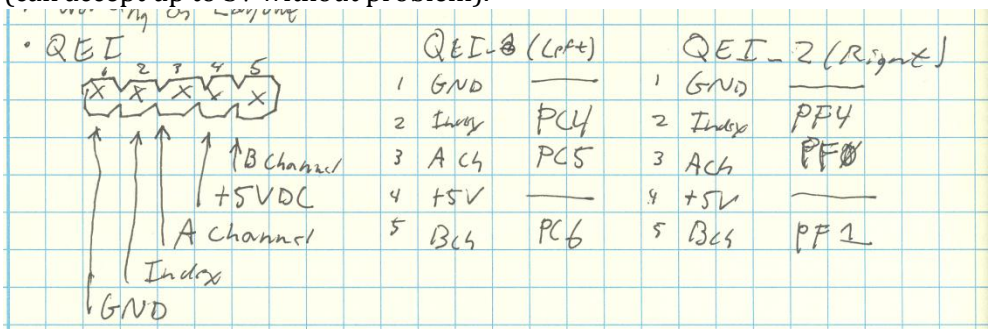

2.7.1.7. Inertial Measurement Unit (IMU) Interface

The IMU (14) provides magnetic heading, yaw rate of rotation, and tri-axis acceleration data via an I²C bus connection (see I²C, section 2.7.1.3). Principle of operation is not provided in this document for MEMS sensors responsible for producing these measurements.

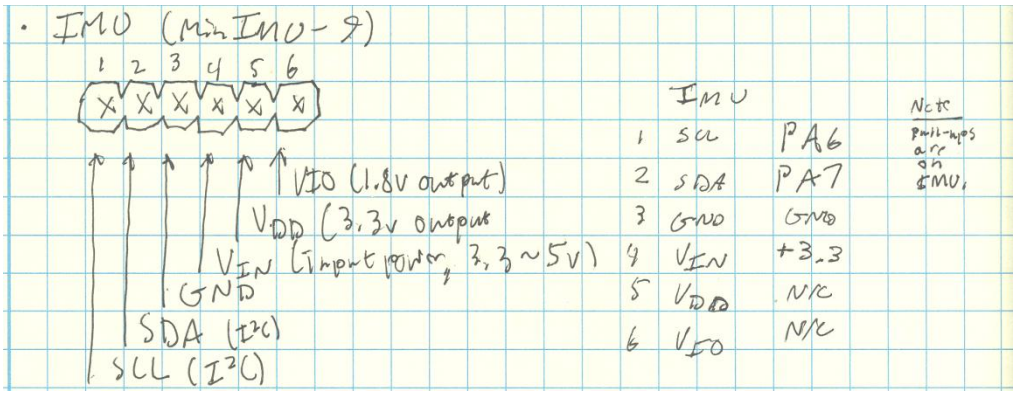

2.7.1.8. Accessory Low-Side Drives

We decided to add a pair of accessory low-side drives to the carrier board, to run loads such as signal lights. N-FETs used are the same model as those used as the power switches in the H-Bridge. Zener diodes were added in reverse bias across the DS junction of the two N-FETs. This is in place to protect against inductive transients if an inductive load is being switched. Gate drive is provided by a pair of pins level translated up to 5v (the level translator used here as a mild gate driver). Pins selected for controlling these low side drives can muxed in the LM4F232 to take their outputs from one of the internal PWM units (i.e. perhaps to fade lights in/out).

The 0.1" pitch header pins used as connectors here are the limiting factor for current, rated to about 1A average.

2.7.2. Layout Constraints

As this board was designed to be produced in-house by the parts shop on their LPKF PCB milling machine, special considerations had to be considered for design. No through holes, including vias, are plated through, making bottom-side-heavy layouts very attractive. Special care was taken to utilize the bottom side as much as possible, minimize use of vias, and the inability to solder pins on most components. In select instances, through hole parts were used expressly to overcome a need for a via.

For your reference, a copy of the main schematic sheet for the carrier board has been attached to the end of this document following the references section as appendix A.

2.7.3. Layout as Sent to Electronics Shop

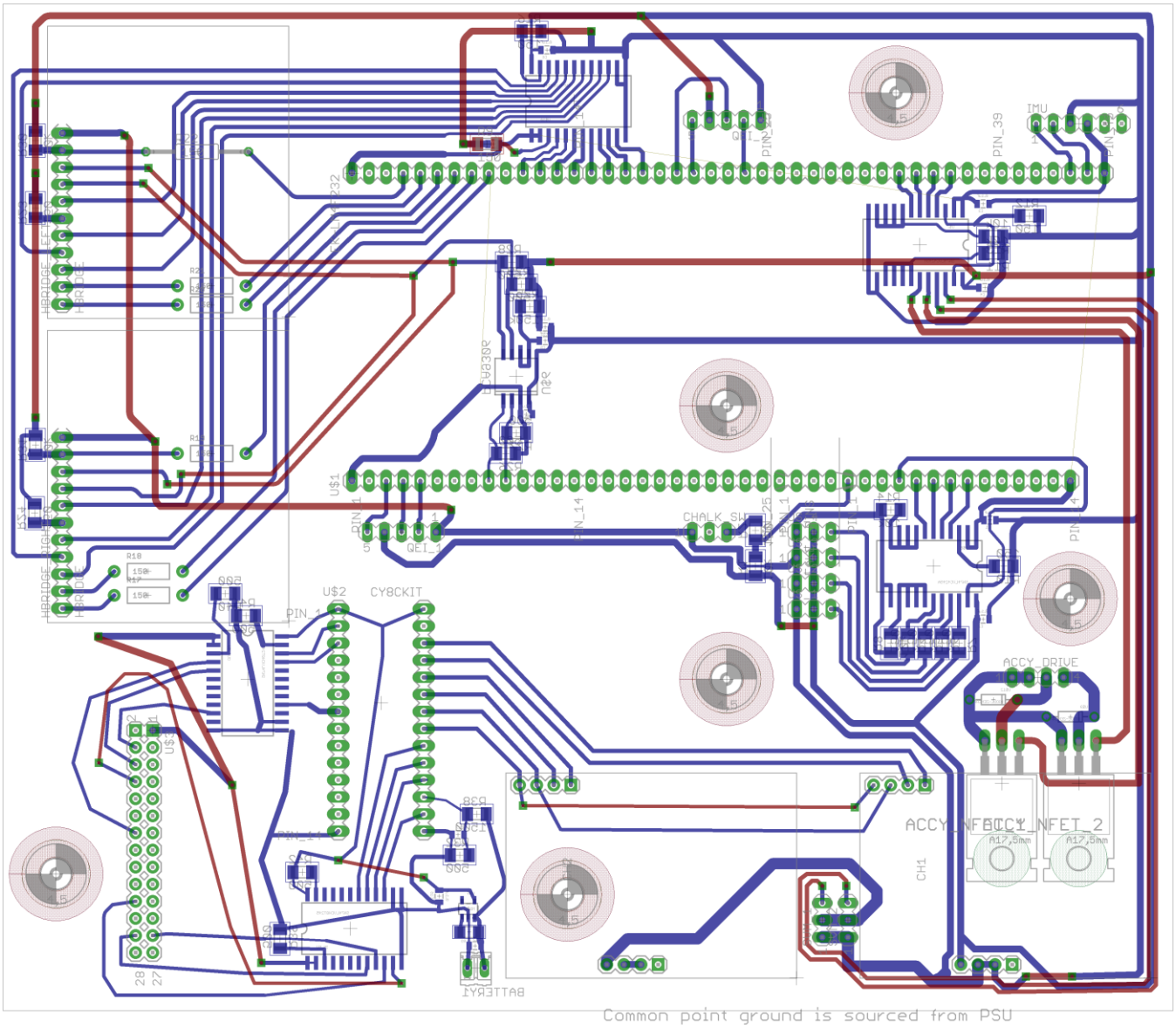

3. Conclusion

3.1. State of the Design

Currently, the power supply unit is completed and ready for use. The revision one H-Bridge is also ready and can be used, though the new revision two H-Bridge with electrical noise abatement strategies is preferable. The supervisor board and motion control board are both in stock and ready, as is the mechanical platform for the robot, ultrasonic sensors, and IMU.

3.2. Future Work

Once the carrier board is received from the parts shop, and parts on order for its construction arrive, work can begin on assembling the carrier board. In addition, all parts for the revision two H-Bridge referred to in section 2.4.2 should arrive within the next week.

Once the carrier board is complete with all it's daughter cards installed, in concert with the Pandaboard, our robot control hardware will be complete. At this point, much software authoring for the supervisor, motion controller, and Pandaboard can begin. Once nay hardware debugging/modification is completed, and sufficient software has been designed and authored to merit first testing, the control board can be mounted on the mobile robot platform and final testing can begin.

REFERENCES

1. **Karavaev, George.** Champaign-Urbana, Illinois : Alex Suchko, 2011.

2. **Midwest Motion Products.** MMP D22-376D-24V GP52-016. *Midwest Motion Products.* [Online] [Cited: 10 25, 2011.] http://www.midwestmotion.com/products/brushed/24VOLT/250-374%20RPM/17-19%20IN-LBS/MMP%20D22-376D-24V%20GP52-016%20specs.pdf.

3. Lead-acid battery. *Wikipedia.* [Online] [Cited: 10 25, 2011.] http://en.wikipedia.org/wiki/Lead%E2%80%93acid_battery.

4. **Power Sonic.** PS-1270. *Power Sonic.* [Online] [Cited: 10 25, 2011.] http://www.power-sonic.com/images/powersonic/sla_batteries/ps_psg_series/12volt/PS-1270_11_Feb_21.pdf.

5. **ON Semiconductor.** NCP3155. *ON Semiconductor.* [Online] [Cited: 09 11, 2011.] http://www.onsemi.com/pub_link/Collateral/NCP3155-D.PDF.

6. Phase margin. *Wikipedia.* [Online] [Cited: 10 25, 2011.] http://en.wikipedia.org/wiki/Phase_margin.

7. **IEEE.** IEEE Code of Ethics. *IEEE.* [Online] [Cited: 10 26, 2011.] http://www.ieee.org/about/corporate/governance/p7-8.html.

8. **Parallax, Inc.** PING))) Ultrasonic Distance Sensor. *Parallax, Inc.* [Online] [Cited: 10 26, 2011.] http://www.parallax.com/Portals/0/Downloads/docs/prod/acc/28015-PING-v1.6.pdf.

9. **Texas Instruments.** EKK-LM4F232 Evaluation Kit with Keil Tools. *Texas Instruments.* [Online] [Cited: 10 12, 2011.] http://www.ti.com/lit/ug/spmu272/spmu272.pdf.

10. —. TPS73633. *Texas Instruments.* [Online] [Cited: 10 12, 2011.] http://www.ti.com/lit/ds/symlink/tps73633.pdf.

11. —. SN74LVC4245A. *Texas Instruments.* [Online] [Cited: 10 16, 2011.] http://www.ti.com/lit/ds/symlink/sn74lvc4245a.pdf.

12. —. INA226. *Texas Instruments.* [Online] [Cited: 10 26, 2011.] http://www.ti.com/lit/ds/symlink/ina226.pdf.

13. **NXP.** PCA9306. *NXP.* [Online] [Cited: 10 16, 2011.] http://www.nxp.com/documents/data_sheet/PCA9306.pdf.

14. **Pololu Corporation.** MinIMU-9 Gyro, Accelerometer, and Compass (L3G4200D and LSM303DLH Carrier). *Pololu Corporation.* [Online] [Cited: 09 26, 2011.] http://www.pololu.com/catalog/product/1264.

APPENDIX A - CARRIER BOARD SCHEMATIC